Available online at www.sciencedirect.com

ScienceDirect

Procedia Structural Integrity 61 (2024) 300–304

Structural Integrity Procedia

www.elsevier.com/locate/procedia

3rd International Workshop on Plasticity, Damage and Fracture of Engineering Materials (IWPDF 2023)

Frictional Sliding Modes using the Maxwell-Slip Model

Tutku Ilgın Ozcan[a], Aydın Amireghbali[a,c], Demirkan Coker[a,b,*]

[a]*Department of Aerospace Engineering, Middle East Technical University, 06800 Ankara, Turkiye*
[b]*METU Center for Wind Energy and Research, Middle East Technical University, 0680 Ankara, Turkiye*
[c]*Currently at: Department of Aerospace Engineering, Samsun University, 55060 Samsun, Turkiye*

Abstract

This study investigates the frictional sliding dynamics occurring at the interface between two bodies in contact by using the Maxwell-slip model at the microscopic scale. The elastic body is modeled as a set of independent mass-spring units that are pulled with a rigid driver moving at a constant speed on top. Coulomb friction law is assumed at the mass-spring level. Initial compressive loading is represented by the degree of Poisson's expansion and its effect on the frictional sliding behavior is examined by using a dynamic solution to the Maxwell-slip model. Both stick-slip behavior and steady state behavior is observed for decreasing compressive loading. Our results show that stick-slip behavior at the macroscopic scale is observed caused by crack-like slip propagation at the microscopic scale at higher compressive loads. Macroscopically diminishing stick-slip behavior is observed for higher initial compressive loading conditions as pulse-like slip propagation through the interface is observed. At the highest initial compressive loading condition, propagation of train of pulses through the interface at the microscopic scale is observed causing a steady sliding behavior at the macroscale.

© 2024 The Authors. Published by Elsevier B.V.
This is an open access article under the CC BY-NC-ND license (https://creativecommons.org/licenses/by-nc-nd/4.0)
Peer-review under responsibility of the scientific committee of IWPDF 2023 Chairman

Keywords: Sliding friction; Maxwell-slip model; Frictional sliding modes; Stick-slip; Steady sliding

1. Introduction

Understanding the relative sliding motion occurring along the interface between two surfaces in contact is important in many fields like tribology, geophysics, and engineering. Examples of frictional sliding are present in a very wide scales from atoms to earthquakes. The factors causing frictional sliding, therefore, are being investigated in many fields. At macroscale, earthquakes are frictional ruptures, i.e. relative sliding motion along the preexisting faults in the Earth's crust. Frictional rupture is characterized by its rupture speed and rupture mode, namely crack-like and pulse-like. In the crack-like mode, each point on the fault continuously slides and has a slip duration comparable to the total rupture duration, whereas in the pulse-like mode, a relatively small propagating region exists where the slip duration of each point on the fault is much shorter than the total rupture duration. The conditions causing pulse-like mode are investigated theoretically, numerically, and experimentally in the literature. There have

* Corresponding author. Tel.: +90-312-210-8230; fax: +90-312-210-4250.
E-mail address: coker@metu.edu.tr

2452-3216 © 2024 The Authors. Published by ELSEVIER B.V.
This is an open access article under the CC BY-NC-ND license (https://creativecommons.org/licenses/by-nc-nd/4.0)
Peer-review under responsibility of the scientific committee of IWPDF 2023 Chairman
10.1016/j.prostr.2024.06.038

been numerous studies in the literature that have focused on the mechanisms that generate pulse-like vs. crack-like behavior. The possible factors include the type of friction law (Brener et al., 2018; Coker et al., 2005; Zheng and Rice, 1998; Lu et al., 2010) fault geometry (Melgar and Hayes, 2017), prestress (Lu et al., 2010), stress barriers or local heterogeneities. Special attention has been paid to the existence of normal stress variation due to bimaterial effect and velocity weakening friction law as a cause of pulse-like propagation along the interface (Thogersen et al., 2021).

In this study, our aim is to investigate the micro-level slippage that leads to macroscopic stick-slip or creep like behavior by using a simple 1D spring-block model, Maxwell-slip model, originally used to provide a friction model to design friction compensators (Chiew et al., 2013; Vo-Minh et al., 2011; Zschack et al., 2012; Rizos and Fassois, 2004; Al-Bender et al., 2005). Assuming Coulomb friction law at the mass-spring level, the effect of initial compressive loading, i.e. prestress, on the instability and sliding modes is investigated by representing the magnitude of the load by the spread of the blocks of the Maxwell-slip model through Poisson's expansion effect. Dynamic solution of the model reveals that for low initial compressive loads, the spring block leads to enlarging sliding region of blocks, i.e. crack-like propagation, which at the macroscale is observed as a stick-slip behavior. We show that as the initial compressive load is increased, the sliding region shrinks from crack-like to a pulse-like region.

2. Method

This section introduces Maxwell-slip model and a dynamic solution to the model. Dynamic solution is used to investigate the effect of Poisson's expansion (due to initial compressive loading).

2.1. Maxwell-slip model

The frictional interface between two elastic bodies in contact is to be modeled with the 1-D Maxwell-slip model shown in Figure 1. The elastic properties of both bodies are embedded into the upper body, and the lower body is modeled as a fixed and rigid substrate. The frictional interface of the global system is represented by the interfaces between the mass blocks of the elastic upper part and the rigid, fixed substrate. The elastic part is composed of N number of blocks of mass m, each connected to a slider on top with a leaf spring that carries only tangential force with the stiffness k. Each mass-spring unit represents the asperities that are far enough from each other at the microscopic level.

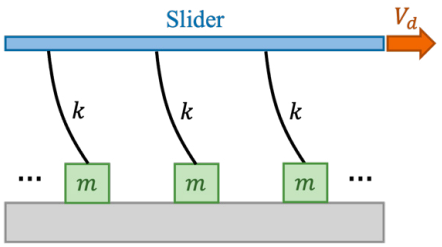


Figure 1. Maxwell-slip model

The slider is moved at a constant velocity, V_d, to initiate the relative sliding motion along the interface. Amontons-Coulomb law is imposed to the system where all blocks have the same local static coefficient of friction, μ_s, that is greater than the local kinetic coefficient of friction, μ_d.

The compression forces, N_c, acting on the blocks are identical, and equal to the normal pressure, p, exerted on the blocks multiplied by the top area, LW, of the mass block over which the pressure acts. The initiation of relative sliding happens when the spring force, F_{sp}, exerted on a mass block exceeds the local static friction force, $f_s = \mu_s N_c$, acting on that block.

2.2. Dynamic solution

A dynamic solution is employed to the Maxwell-slip model to investigate the Poisson's expansion (initial compressive load) effect on the friction mode and the frictional sliding behavior. When an elastic body is compressed against a rigid flat surface, it expands laterally because of Poisson's expansion. By introducing a linear and anti-symmetric distribution to the initial lateral positions of the mass blocks, the Maxwell-slip model mimics the spreading behavior caused by Poisson's expansion. The linear distribution with a high slope, i.e., the end blocks have larger lateral initial extensions, corresponds to a higher initial compressive load acting on the body. Similarly, a smaller slope corresponds to a lower initial compressive load acting on the body.

Initiation of sliding is started with the constant speed motion of the slider. The traction force is the sum of the spring forces on the blocks and the macroscopic friction force is the sum of the microscopic friction forces exerted by the substrate on the blocks. The driver is not stopped, and the sliding motion of the mass blocks is tracked, so the spring force on a mass block includes inertial force during sliding. As a result, the friction and traction forces differ from each other. The contribution of the stuck block is the

same to both traction and friction forces; however, the contribution of a sliding block to traction and friction forces is not the same. The equation of motion of a single block of mass m under Coulomb's friction law that is pulled with a spring of stiffness k by a driver that is moved at a constant velocity V_d is:

$$m\ddot{x}(t) = F_{sp} - f_d = k\big(V_d t - x(t)\big) - f_d$$

The solution, $x(t)$, can now be obtained by solving the EOM of the block with $x(0) = d$ and $\dot{x}(0) = 0$ initial conditions. Subsequently, the friction and traction forces can be found by calculating the forces on the blocks.

3. Results

The results of the Maxwell-slip model are presented in this section for different slopes for the initial lateral position distribution causing different maximum initial lateral position. The plots of macroscopic coefficient of friction and the local movement of blocks with respect to time are presented. Also, to identify the frictional sliding modes, the sliding velocity of the blocks is plotted at selected times.

Westerly granite has been chosen as the material. Young's modulus and Poisson's ratio of Westerly granite are 70 GPa and 0.25, respectively. The pressure wave speed is 5.1 km/s and the shear wave speed is 2.23 km/s for westerly granite having a density of 2,691 kg/m^3. For the individual blocks, the microscopic static and dynamic coefficients of friction are assumed to be 0.8 and 0.7, respectively. The driver is moved at a constant velocity of $V_d = 1\ mm/s$. The number of blocks is taken as 500, and all the blocks are identical with the length L, height H, and width W being 1 μm. The spring stiffness is calculated from, $k = GLW/H$, and the normal force applied to each block is calculated from $N_c = pLW$, where p is the pressure and is taken as 1 MPa. The time step size is selected to be 0.01 s.

The dynamic solution to the Maxwell-slip model reveals three propagation types, namely, crack-like, pulse-like, and train of pulses. These modes appear depending on the slope of linear initial lateral position distribution, i.e., when the model is under different initial compressive loads. The results showing these three modes are presented separately, each with three figures, plot (a) showing the macroscopic coefficient of friction with time, plot (b) showing the sliding block percentages in black and the sliding block indices in red as a function of time, and plot (c) showing the sliding velocity of the blocks, i.e., particle velocity, at different prescribed times to capture the mode of propagation.

The results of the first case in which the maximum initial lateral position of the end blocks is chosen as $x_{max} = 10^{-13}\ m$ corresponding to the lowest initial compressive load are presented in Figure 2. Figure 2.a shows that the macroscopic (apparent) coefficient of friction climbs elastically to the microscopic static coefficient of friction value (shown with a horizontal gray line) at 2.85e-08 seconds and continues with a stick-slip behavior. Sliding initiates after the macroscopic COF reaches the microscopic static COF value followed by a steep drop in the apparent coefficient of friction in a very small time interval of 0.1e-08 seconds. In Figure 2.b sliding blocks are shown in red where 100% of the blocks slide and then reach a full stop and 0% of the blocks slide after the slip region. All slippages along the interface take place in a very small time interval within the force-drop. When we look at the sliding velocities of the blocks in the time interval indicated by the dashed lines in Figure 2.a (time interval between 2.8501e-08 s and 2.8998e-08 s), we observe a growing slipping region along the interface, similar to a crack-like propagation (Figure 2.c).

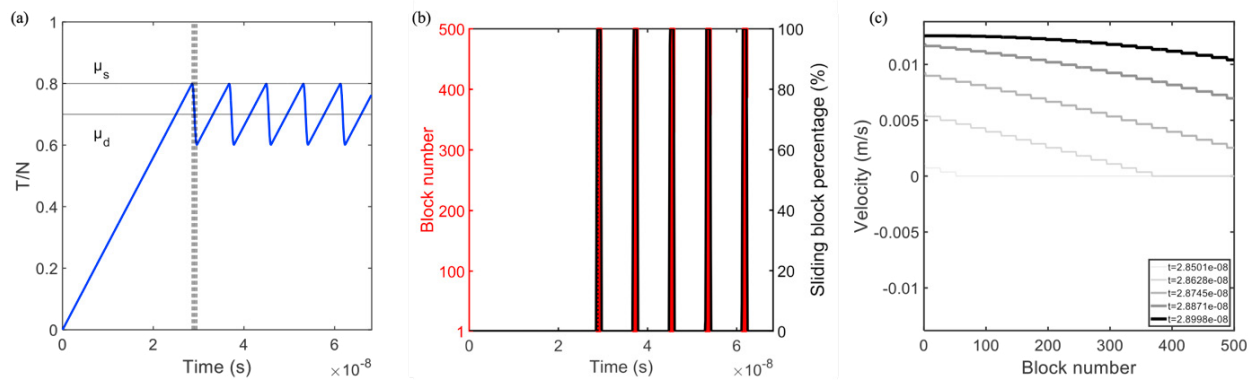


Figure 2. Case (i): $x_{max} = 10^{-13}$ (a) Coefficient of friction as a function of time. (b) Sliding block number and sliding block percentage in time. (c) Sliding velocity of the blocks along the interface at different times shown with dashed lines in (a) and (b).

In the second case, the maximum initial lateral position of the blocks is increased to $x_{max} = 10^{-12}\ m$ representing an increase in the compressive load. Here we observe that stick-slip behavior appears again but with a smaller amplitude. Figure 3.a shows

that the apparent coefficient of friction climbs elastically to a value of 0.78, which is smaller than the microscopic static coefficient of friction value (shown with a horizontal grey line) at 2.79e-08 seconds and continues with a lower amplitude stick-slip behavior at a slip time of 0.24e-08 seconds. In Figure 3.b, 51.6% of the blocks slide and then reach a full stop as seen in the first case. A single slip-pulse propagation along the interface is observed in Figure 3.c which shows several snapshots of the sliding velocities of the blocks in the time interval indicated by the dashed lines in Figure 3.a. As can be seen, starting from the left-end, a single slip-pulse heals the interface behind it as it travels through the interface with time.

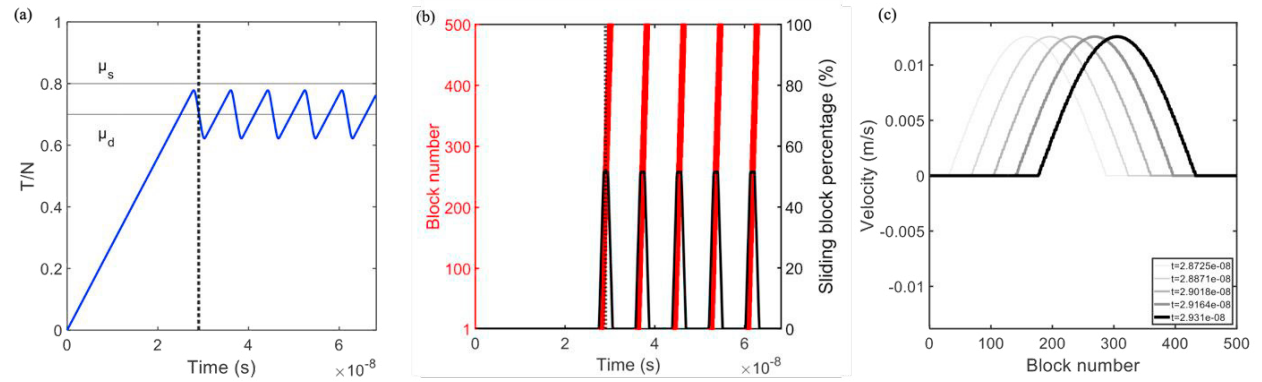


Figure 3. Case (ii): $x_{max} = 10^{-12}$ (a) Coefficient of friction as a function of time. (b) Sliding block number and sliding block percentage in time. (c) Sliding velocity of the blocks along the interface at different times shown with dashed lines in (a) and (b).

In the third case, the maximum initial lateral position of the blocks is further increased to $x_{max} = 2.82x10^{-11}\ m$ representing further increase in the compressive load. It is observed that stick-slip behavior seen in previous cases completely transitioned to steady sliding behavior shown in Figure 4.a. A non-linear presliding region is observed until global sliding occurs (at $t = 4.98e-08\ s$) when the macroscopic COF value approaches the microscopic dynamic COF value. In Figure 4.b, at the beginning, a single slip pulse travels then it is followed by other slip pulses with time. Multiple slip pulses propagating along the interface are observed in Figure 4.c which shows the sliding velocities of the blocks in the time interval indicated by the dashed lines in Figure 4.a. It is observed that the multiple slip pulses, i.e., a train of pulses, prevent the stick phase to occur at the macro-level.

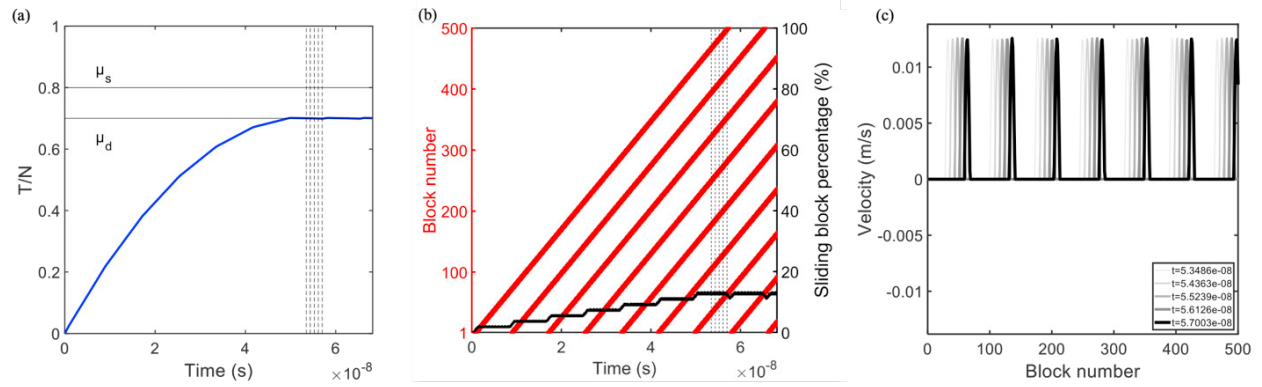


Figure 4. Case(iii): $x_{max} = 2.82x10^{-11}\ m$ (a) Coefficient of friction as a function of time. (b) Sliding block number and sliding block percentage in time. (c) Sliding velocity of the blocks along the interface at different times shown with dashed lines in (a) and (b).

4. Conclusion

In this study, we employed the dynamic solution of the Maxwell-slip model at the microscale to explore both the stick-slip and steady sliding phenomena at the macroscale. We investigated the effect of compressive loading through modeling the initial lateral positions of the blocks on the crack-like and pulse-like sliding regimes. Our results showed that an increase in the initial compressive loading led to a transition in slip propagation at the microscale, progressing from a crack-like mode to a pulse-like mode and eventually to train of pulses. Crack-like and single pulse-like frictional sliding modes lead to a stick-slip behavior at the macroscopic scale and train of pulses sliding mode leads to a steady sliding behavior at the macroscopic scale. These observations are similar to those observed in the finite element simulations of Coker et al. 2005, carried out under dynamic impact of similar

plates and using a rate- and state- friction model. Consequently, in this paper we show that by introducing only prestress and bimaterial effect, different frictional sliding modes can be captured along the interface.

References

Al-Bender, F., Lampert V., and Swevers J., 2005. The generalized Maxwell-slip model: A novel model for friction simulation and compensation. IEEE Transactions on Automatic Control, 50 (11), 1883-1887.

Brener, E. A., Aldam, M., Barras, F., Molinari, J. F., Bouchbinder, E., 2018. Unstable Slip Pulses and Earthquake Nucleation as a Nonequilibrium First-Order Phase Transition. Physical Review Letters, 121 (23), 234302

Chiew T. H., Jamaludin Z., Bani Hashim A. Y., Rafan N. A., and Abdullah L., 2013. Identification of friction models for precise positioning system in machine tools. Procedia Engineering, 53, 569-578.

Coker D., Lykotrafitis G., Needleman A., and Rosakis A. J., 2005. Frictional sliding modes along an interface between identical elastic plates subject to shear impact loading. Journal of Mechanics and Physics of Solids, 53 (4), 884-922.

Lu, X., Lapusta, N. and Rosakis, A.J., 2010. Pulse-like and crack-like dynamic shear ruptures on frictional interfaces: experimental evidence, numerical modeling, and implications. International Journal of Fracture, 163, 27-39.

Melgar, D., and Hayes, G. P., 2017. Systematic Observations of the Slip Pulse Properties of Large Earthquake Ruptures. Geophysical Research Letters, 44 (19), 9691-9698.

Rizos D. D., and Fassois S. D., 2004. Presliding friction identification based upon the Maxwell-slip model structure. Chaos, 14 (2), 431-445.

Thogersen, K., Aharonov, E., Barras, F., and Renard, F., 2021. Minimal model for the onset of slip pulses in frictional rupture. Physical Review E, 103, 052802.

Vo-Minh T., Tjahjowidodo T., Ramon H., and Van Brussel H., 2011. A new approach to modeling hysteresis in a pneumatic artificial muscle using the Maxwell-slip model. IEEE/ASME Transactions on Mechatronics, 16 (1), 177-186.

Zheng, G., and Rice, J. R., 1998. Conditions under which velocity-weakening friction allows a self-healing versus a cracklike mode of rupture. Bulletin of the Seismological Society of America, 88 (6), 1466-1483.

Zschack S., Bichner S., Amthor A., and Ament C., 2012. Maxwell-slip based adaptive friction compensation in high precision applications. IECON 2012, (Montreal, QC, Canada), 38th Annual Conference on IEEE Industrial Electronics Society.